

Viscous droplet breakup in narrow pore systems

Tobias Wollborn^{*1}, Laura Luhede¹, Alexander Schulz^{1,2}, Teena Tom Puthenveetil¹, Udo Fritsching^{1,2}

¹Leibniz Institute of Materials Engineering - IWT, D-28359 Bremen, Germany

²Particles and Process Engineering, University of Bremen, Germany

*Corresponding author: wollborn@iwt.uni-bremen.de

Abstract

A Volume-of-Fluid method formulation within OpenFOAMS InterFoam solver was implemented. This model enables the calculation of local shear and strain conditions (stress tensor) at the interface of a liquid-liquid system. With this extension the stress residence time behavior at the liquid-liquid interface in idealized pore structures and elementary flow constrictions has been analyzed. Parameters were varied by the pore geometry and capillary number. The parameters influence on the droplet deformation and breakup process is analyzed to derive the main stress related mechanisms for droplet breakup. The simulation procedure was extended to real membrane pore geometries (CT-scans) and compared to the stress conditions and break up mechanisms received from the idealized pore geometries. Local and integral stress conditions gives insight of the geometry and time dependent droplet deformation and breakup process enabling new approaches in membrane design.

Keywords

Shear stress, droplet breakup, microporous structures, CFD

Introduction

The use and production of high quality emulsion with a fine and homogeneous droplet size distribution is a key factor in several industries, i.e. pharmaceutical and food technology [1], [2]. In particular the premix emulsification process allows the adjustment of the droplet size distribution according to the membrane and pore structure. Furthermore it is a low shear process suitable for shear sensitive media (i.e. biological systems). The influence of the process parameters on the final product (droplet size distribution) has already been well investigated in literature. Egidi et al. [3] investigated the effect of pore spacing on the droplet generation process, whereas Hornig and Fritsching [4] correlate the structural properties of the membrane with the emulsification behavior. A numerical model representing the droplet generation and interacting process was designed by Krause et al [5]. However, the mechanisms regarding the droplet deformation and breakup within the membrane structure are still unknown. The deformation and breakup process is determined by local shear and strain stresses. Local stress peaks, but also frequently stressing (stress-residence-time) of the droplet interface may cause breakup of the droplet. Furthermore shear sensitive emulsifiers (i.e. proteins) are affected by local and time dependent stress distributions, which may have an effect on the quality of the final product. Hence, in this work numerical investigations with the Volume-of-Fluid-Method were performed to understand stress related breakup mechanisms in microporous structures.

Material and methods

Numerical procedure:

The numerical investigations have been performed by using the interFoam solver of the open computational fluid dynamics (CFD) software OpenFOAM, which is based on the volume-of-fluid (VOF) method. The fluid phases (disperse and continuous) are described by the α -value with $\alpha_{disp} = 0$ and $\alpha_{conti} = 1$. Based on the method the boundary between both phases is smeared. Hence, the interface is defined to a value of $\alpha_{int} = 0.5$. The governing equations (transport, continuity and momentum) are solved using a double precision solver. A PISO loop is used to achieve the coupling between velocity and pressure terms, which is adapted to the momentum equation for the interphase solver. For the solution of the convective term second order divergence schemes are used. In the simulation a Cartesian mesh is used. Due to the sensitivity of the solution of the partial differential equation system to the Courant number the time steps are adapted to a maximum Courant number of $Co_{max} = 0.1$. This results in time steps in the range of 10^{-8} and 10^{-6} s.

For the calculation of the interfacial shear stress the orientation of the interface has to be taken into account. Hence, the interface normal is calculated by using the alpha gradient pointing in the direction of increasing values. This leads to the expression

$$\vec{n}_{int,\perp} = \frac{\nabla(\alpha)}{|\nabla(\alpha)|} \quad (1)$$

Together with the velocity gradient tensor $D = \text{grad}(u) + \text{grad}(u)^T$ the interfacial shear stress results in

$$\tau_{int} = \mu_{int} \vec{n}_{int,\perp} D_{int} \quad (2)$$

Here, μ_{int} is the dynamic viscosity at the interface. The equations have been implemented in the interFoam solver.

Numerical setup:

For the evaluation of the stress related droplet breakup mechanisms, a simplified single is designed [6]. It consist a tube channel with abrupt reduction of the diameter. This leads to deformation and stressing of the droplet similar to real pore structures. The inlet tube diameter has been set to $d_{inlet} = 1$ mm and the pore diameter to $d_{pore} = 0.2$ mm. The length of the pore channel is $l_{pore} = 6$ mm. A mesh based on an O-grid with a refined layer at the wall due to expected high velocity gradients has been created. This results in a resolution of 1.7×10^6 cells. The stress residence time in complex pore structures has been evaluated by a CT-Scan of a real membrane structure (type P2, Robu) with a mean pore diameter of $d_{pore,P2} \approx 70 \mu\text{m}$. The dimensions of the scan are $1.4 \times 2.0 \times 1.6$ mm with a porosity of $\varepsilon = 0.31$. Also here a Cartesian mesh is used with a mesh refinement at the pore walls. The resulting mesh consists 7.6×10^6 cells. As boundary condition a constant velocity and constant pressure inlet is used, respectively. At the wall the no slip condition is set for the velocity.

Both setups have been checked for the mesh independence of the solution at different refinement levels by comparing the means of velocity and pressure profiles. Mesh independence for the generic pore structure has been achieved at 1.2×10^6 cells. For the complex pore structure even for the finest resolution used (7.6×10^6 cells) no full mesh independence has been achieved. This is due to the very complex branching of the pore network, which cannot not be completely resolved. Hence, a full mesh independence has been estimated to resolution up to 10^8 cells. This is computationally not realizable. However, validation studies of the droplet breakup in a previous work [6] show that the droplet behaviour can be represented with the current mesh resolution. Also the changes of the mass flux between the investigated refinement steps are very small ($\approx 1\%$). Therefore it is assumed that the mesh depended behavior results from the insufficient resolution of the pore network, but not from the numerical solution. Therefore a compromise between resolution of the pore structure and computational effort is required.

Material parameters:

The relevant material parameters were experimentally determined. As disperse phase MCT (middle-chain triglycerides, Endima GmbH) oil is considered. As continuous phase water is used. The viscosity is measured by using a cone and plate rheometer setup (Bohlin CVO 100). The viscosity values were determined to $\mu_{disp} = 0.029$ kg m⁻¹ s⁻¹ and $\mu_{disp} = 10^{-3}$ kg m⁻¹ s⁻¹. The MCT density has been analyzed by the mass volume ration, resulting in $\rho_{disp} = 952 \pm 3$ kg m⁻³. The density of water is set to $\rho_{cont} = 1000$ kg m⁻³. The surface tension has been measured via pendant drop measurements and results in $\sigma = 0.024$ N/m. In technical applications a contact angle $> 90^\circ$ for the disperse phase is typically used, which is provided by sintered glass membranes [7], [8]. The contact angle is set to a common value of $\Theta_{cont} = 30^\circ$ for the continuous phase ($\Theta_{disp} = 150^\circ$ for the disperse phase). The effect of contact angle is investigated in a future work of this study.

Results and discussion

For the determination of the droplet breakup mechanism simulations for the simplified pore have been performed in a recent study [6] under variation of the capillary number Ca:

$$Ca = \frac{\mu_{disp} \bar{u}_{pore}}{\sigma} \quad (3)$$

μ_{disp} is the dynamic viscosity of the disperse phase, \bar{u}_{pore} is the mean pore velocity and σ is the surface tension. A qualitative result of the droplet deformation at different capillary numbers Ca is shown in Figure 1. The relative interfacial stress conditions are indicated by the color bar.

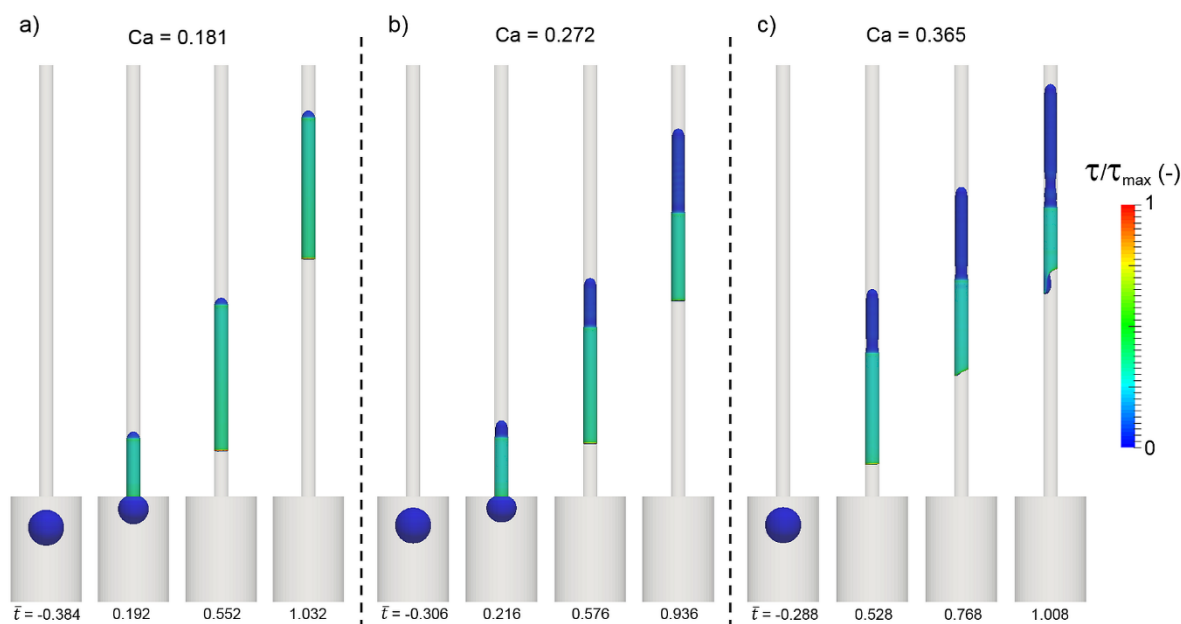


Figure 1. Droplet deformation in a simplified pore structure at different capillary numbers Ca . The color bar indicates the interfacial stress during deformation. [6]

At the lowest capillary number (a) the droplet shows a slug-like behaviour. After entering the pore structure no further deformation is observed. With an increase of the capillary number (b) further deformation of the droplet occurs. A detachment of the droplet from the pore wall is induced. The length of the detached area increases continuously with residence time and movement in the pore channel. No droplet breakup can be observed at this flow condition. At the highest capillary number (c) the droplet detachment from the pore takes place faster. Furthermore a constriction of the droplet at the detached area is observed, which finally leads to breakup of the droplet. At the bottom of the droplet further deformation effects are initialised in terms of the formation of lip. This is due to asymmetric contact line instabilities with the pore wall. As already stated in [6] the effect is similar to the splashing effect of droplets after impact as investigated by Frohn and Roth [9]. From these observations general breakup mechanisms are derived as described in [6]: i.) breakup is initialized by the detachment from the pore wall due to contact line instabilities, ii.) deformation of the detached part of the droplet caused by shear and strain stress histories, and iii.) breakup of the droplet as a consequence of local constrictions.

The resulting time dependent shear stress distributions from the droplet deformation behaviour in Figure 1 are shown in Figure 2. For each droplet the stress is separated in liquid interface stress (disperse-continuous interface) and wall interface stress (disperse-wall interface). The dimensionless time t_0 describes the time where the first cell of the droplet enters the pore channel, the time t_{max} describes the time where the first cell of the droplet exits the pore channel. Hence, the stress distribution always considers the whole interface of the droplet.

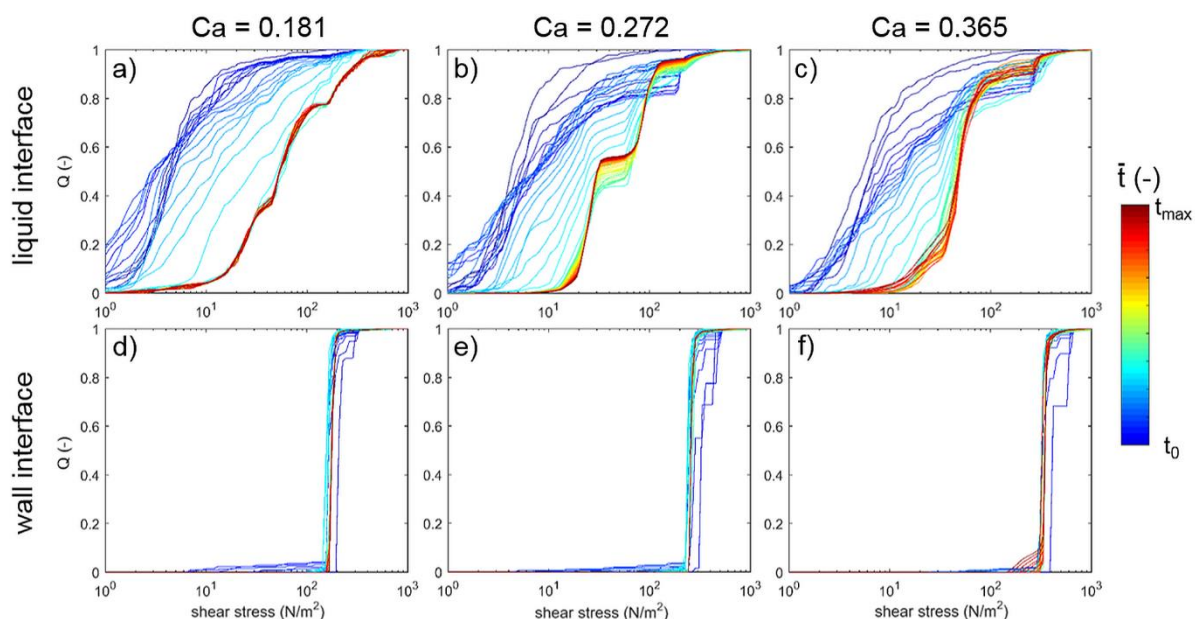


Figure 2. Cumulative interface shear stress distribution in a simplified pore structure at different capillary numbers Ca split into liquid interface (disperse-continuous, a-c) and wall interface (disperse-wall, d-f) stress. [6]

The stress distribution at the liquid interface (a-c) shows a broad distribution shifting to higher values over time. This is due to the entering process of the droplet in the pore channel. At the lowest capillary number (a) the stress distribution remains constant after full entering of the droplet in the pore channel. This indicates no further deformation in the channel as already stated in Figure 1 a). At higher capillary number (b and c) further changes of the stress distributions after full entering of the droplet is shown. This results from the further deformation of the droplet described in Figure 1 and indicates a direct connection of the interface stress distribution and the droplet deformation process. Furthermore the distributions in a-c show a characteristic shape at each capillary number. The different segments describe different stress sectors, which can be connected to certain regions on the droplet interface. In contrast to the liquid interface the distribution at the wall interface (d-f) shows a narrow distribution and no significant change over time compared to the liquid interface. This indicates that the droplet deformation and only takes place at the liquid interface and that the stress distribution at the wall is irrelevant for the breakup process. A detailed analysis of the development of the stress distribution and connection to droplet interface regions has been performed in [6].

In a next step the droplet deformation and breakup process in complex pore structures is investigated. The droplet has been dispersed in the porous network at different inlet pressures. In Figure 3 a qualitative analysis of the droplet dispersion process is shown.

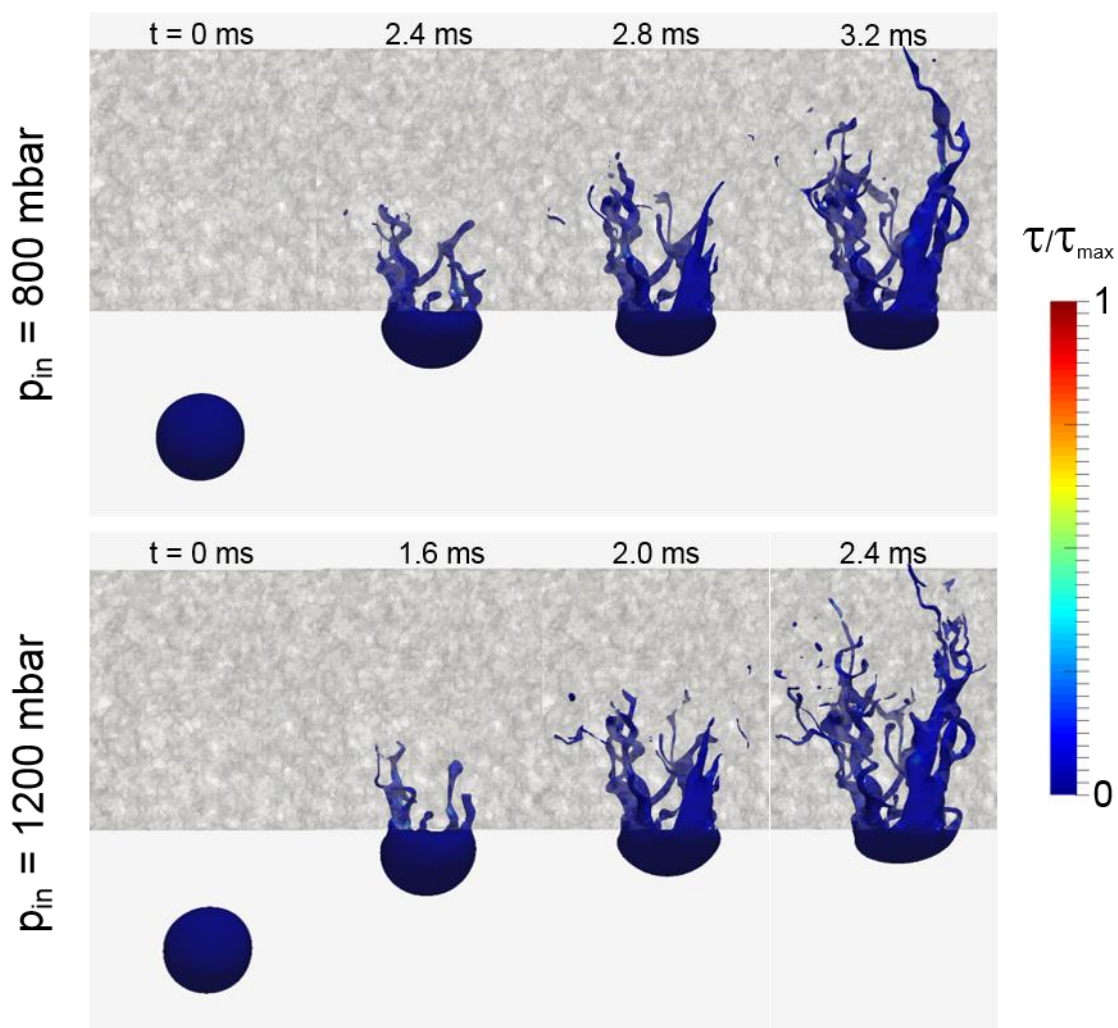


Figure 3. Droplet deformation in a complex pore structure at different inlet pressures p_{in} .

Once the droplet arrives the membrane the droplet breaks up in different pore channels leading to complex breakup events. Further breakup occurs by splitting at branches and by flow induced stretching and constriction of the droplet. This process is similar to the breakup process shown in Figure 1. The comparison in Figure 3 shows that there are no qualitative differences between the two inlet pressures, but dispersion takes place faster at $p_{in} = 1200$ mbar. This is due to the higher driving force (inlet pressure) and the corresponding higher flow velocities.

For a quantitative analysis of the interfacial stress conditions during breakup in complex microporous structure the shear stress distributions at liquid and wall interface are shown in Figure 4.

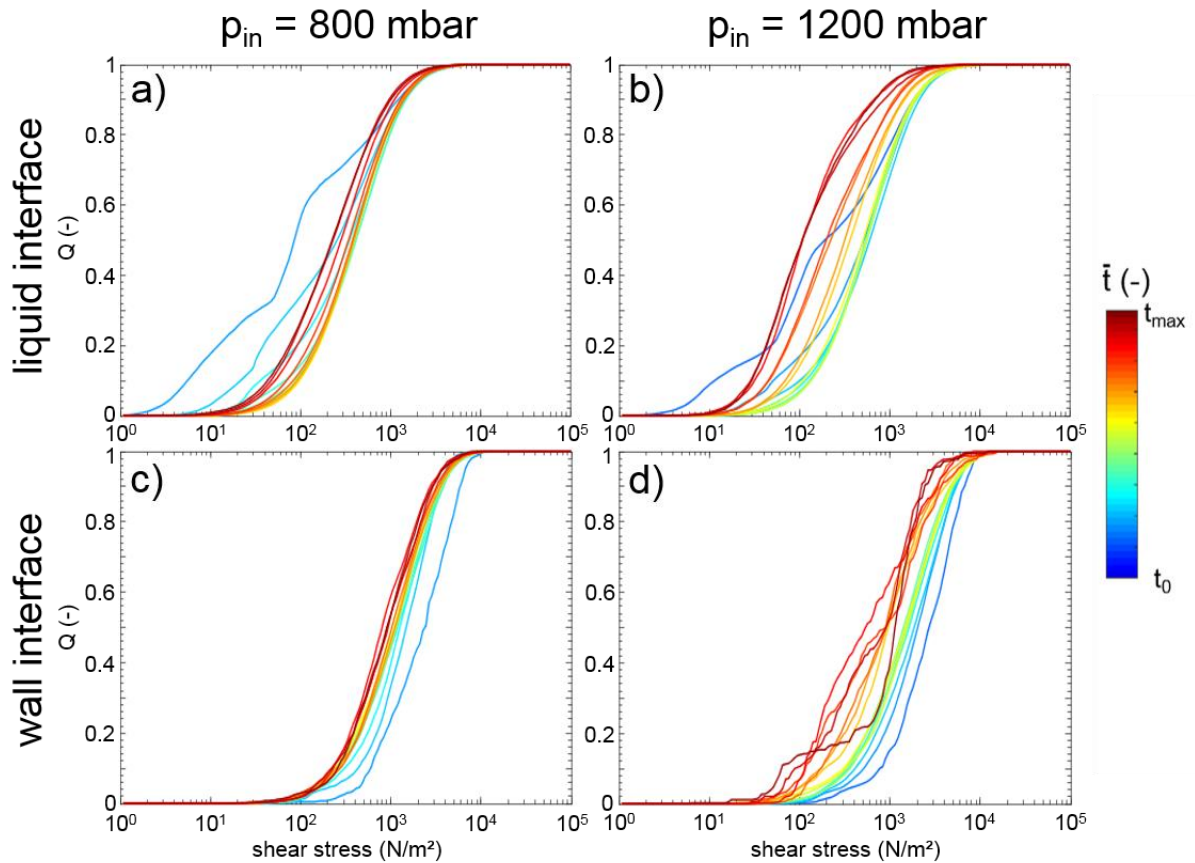


Figure 4. Cumulative interface shear stress distribution in a complex pore structure at different inlet pressures p_{in} split into liquid interface (disperse-continuous, a-b) and wall interface (disperse-wall, c-d) stress.

At the lower pressure (a) the liquid interface stress shows a broad distribution over three orders of magnitude similar to the liquid interface in Figure 2. Also there is only a slight shift over time after entrance indicating only few breakup events in the pore channel. At higher pressure (b) the distribution shifts more clearly to lower values over time. This indicates more deformation and breakup event within the pore channels compared to a), which are hardly visible in Figure 3. Characteristic stress peaks are not present at both pressures. This is due to multiple deformation and breakup events occurring in parallel. At the wall interface the stress shows a more narrow distributed character compared to the liquid interface over two orders of magnitude. This is also similar to Figure 2, but in the simplified structure the distribution is within one order of magnitude. The reason for this is that in the simplified structure droplet deformation is investigated in only one pore channel. In the complex structure deformation occurs in multiple pore channels with different diameter and flow velocities. This leads to different shear gradients and hence to a broader distribution. A similar behaviour can be seen at the higher pressure (d), but here a larger shift of the distribution occurs over time. This is explained by the presence of more deformation and breakup events. The comparison of droplet dispersion in simplified and complex pore structures shows that similar stress effects can be observed, a broader stress distribution at the liquid interface and stronger shift of the distribution due to more breakup events. This approves that the stress related breakup mechanisms derived in [6] enables the stress related characterization of the droplet dispersion in complex pore structures.

Conclusions

The droplet deformation and breakup process and the corresponding interfacial stress distributions have been simulated in simplified and complex pore structures. For the simplified structures general stress related droplet deformation and breakup mechanisms have been derived and a characteristic shape of the stress distributions indicating different stress regions at the droplet interface has been identified for a range of capillary numbers. The separation of liquid and wall interface stress shows that only the liquid interface stress distribution is relevant for the deformation process. The comparison to complex pore structures shows that a similar characteristic stress behavior can be derived. This indicates deformation and breakup processes in the complex pore networks comparable to the simplified pore channel. These findings show that the approach of simplified pore structures is able to characterize and understand the droplet deformation and breakup process in complex structures and to quantify the corresponding interfacial shear stress conditions. This allows a deeper understanding of the mechanisms occur

during droplet dispersion in porous structures enabling new opportunities in membrane design for the emulsification process.

Acknowledgements

This project has been funded by the German Research Foundation (DFG) within the SPP 1934 “DiSPBiotech” (Tobias Wollborn) under Grant No. FR 912/40-1 and the MIMENIMA Graduate School (Laura Luhede and Alexander Schulz) at the University of Bremen. The resources for the numerical calculations have been provided by The North-German Supercomputing Alliance (HLRN) under Grant No. hbi00036/hbi00037. The computer tomograms have been generated at the Institut für Strömungsmechanik (Technische Universität Dresden) (S. Günther, Professor S. Odenbach) within the graduate school 1375 PoreNet.

Nomenclature

Ca	Capillary number [-]
d	diameter [mm]
D	velocity gradient tensor [s ⁻¹]
$\vec{n}_{int,\perp}$	interface normal [-]
l	length [mm]
u	velocity [m s ⁻¹]
p _{in}	inlet pressure [mbar]
t	time [s]
t _{max}	residence time of droplet in pore [s]
α	continuous phase component fraction [-]
Θ	contact angle [°]
τ	shear stress [N m ⁻²]
μ	dynamic viscosity [kg m ⁻¹ s ⁻²]
ρ	density [kg m ⁻³]
σ	surface tension [N m ⁻¹]

References

- [1] Dalglish, D. G., 2006, Food Hydrocoll., 20, 415-422.
- [2] Vladisavljević, G. T., and Schubert, H., Desalination, 144, pp. 167-172.
- [3] Egidi, E., Gasparini, G., Holdich, R. G., Vladisavljević, G. T., Kosvintsev, S. R., 2008, J. Membr. Sci., 323, pp. 414-420.
- [4] Hornig, N., and Fritsching, U., 2016, J. Membr. Sci., 514, pp. 574-585.
- [5] Krause, F., Li, X., Fritsching, U., 2016, Appl. Comp. Fluid, 5, pp. 406-416.
- [6] Wollborn, T., Luhede, L., Fritsching, U., 2019, Phys. Fluids, 31, 012109.
- [7] Schröder, V., 1999, „Herstellen von öl-in-Wasser-Emulsionen mit mikroporösen Strukturen.“
- [8] Lambrich, U., Schubert, H., 2005, J. Membr. Sci., 257, pp. 76-84
- [9] Frohn, A., Roth, N., 2000, “Dynamic of droplets”.